Photocatalytic and Magnetic Properties of TiO_2 Micro- and Nano- Powders decorated by Magnetic Cocatalysts

Tatiana Gegechkori
Department of Condensed Matter Physics, Andronikashvili Institute of Physics, Ivane Javakhishvili Tbilisi State University, Georgia
tatagegechkori@yahoo.com

Grigor Mamniashvili
Department of Condensed Matter Physics, Andronikashvili Institute of Physics, Ivane Javakhishvili Tbilisi State University, Georgia
mgrigor@rocketmail.com

Tornike Gagnidze
Department of Condensed Matter Physics, Andronikashvili Institute of Physics, Ivane Javakhishvili Tbilisi State University, Georgia
tornike.gagnidze@tsu.ge

Malkhaz Nadareishvili
Department of Condensed Matter Physics, Andronikashvili Institute of Physics, Ivane Javakhishvili Tbilisi State University, Georgia
malkhaz.nadareishvili@tsu.ge

T. Zedginidze
Department of Condensed Matter Physics, Andronikashvili Institute of Physics, Ivane Javakhishvili Tbilisi State University, Georgia
tinikozedginidze@yahoo.com

Received: 29 July 2023 | Revised: 18 August 2023 | Accepted: 19 August 2023

 DOI: https://doi.org/10.48084/etasr.6244

ABSTRACT

In this paper, photocatalytic TiO_2 micro- and nano-powders coated by Ni and Co nanoclusters were prepared by the original electroless deposition method. The magnetic properties of Ni and Co nanoclusters decorating TiO_2 grains were studied by the magnetometry measurements of the temperature dependence of magnetization. Their optical spectroscopy measurements showed a significant increase in light absorption by Ni and Co coated TiO_2 nanopowders. The photocatalytic properties of the obtained magnetic nanopowders were studied with Electron Paramagnetic Resonance spectroscopy as well.

Keywords-titanium dioxide; photocatalysis; magnetic clusters; magnetometry; optical spectrometry

I. INTRODUCTION

Hydrogen is a very attractive clean energy source. The use of hydrogen as an energy source has several advantages, such as good energy conversion effectiveness, ability to be produced from water with zero emissions, and different storage options. The product of hydrogen combustion is water and therefore produces no pollutants. The sun's energy can split water into hydrogen and oxygen in the presence of catalysts in a reaction called photocatalysis. Photocatalytic water splitting using semiconducting catalysts has received much attention and is a subject of active research. One of the most promising semiconductor photocatalysts is TiO_2 due to properties such as high photocatalytic activity, excellent incident photoelectric conversion efficiency, photostability, chemical stability, corrosion resistance, low price and nontoxicity [1-5]. The photocatalytic reaction proceeds as follows. Absorbed into

TiO_2, which is a semiconductor and has an energy gap of 3.2 eV between the valence and conduction bands, a sunlight photon with suitable energy creates an electron-hole pair. Having reached the TiO_2 surface, the produced electron and holes interact with water molecules and cause their splitting into hydrogen and oxygen [6].

As mentioned above, the photocatalytic reaction occurs on the surface. Therefore, the photocatalysts are usually used in the form of powders in order to increase the surface area. Therefore, photocatalytic nanopowders are characterized by higher activity than photocatalytic thin films [7]. However, in this case, another problem emerges: on the surface of small particles, the annihilation of electron-hole pairs is very fast, and they have no time to participate in the reaction. The high recombination rate of photogenerated electron and hole pairs in TiO_2 reduces quantum yield and photocatalytic activity, respectively. To circumvent the fast electron-hole annihilation, cocatalist clusters of various substances are deposited on the TiO_2 grain surface. The clusters capture electrons and holes and hinder their annihilation. This process is schematically illustrated in Figure 1.

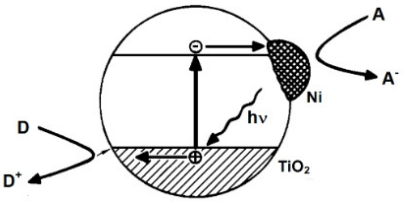

Fig. 1. Electron-hole pair production in the cluster-deposited particles of TiO_2/Ni powder under the effect of sunlight quanta and their interaction with surrounding molecules.

In this paper, we are exploring ways to improve the photocatalytic properties of TiO_2 through the coating of TiO_2 nanoparticles by various metal clusters using the results of [8-10] and some recent experiments. First of all, the preparation and characterization of Ni and Co coated TiO_2 nanoparticles will be described and their magnetic properties and photocatalytic activity under UV-V will be investigated. The main contribution of the current paper is in the development of a new, low-temperature chemical technology for the deposition of magnetic nanosized cocatalysts on the surfaces of TiO_2 nanoparticles. A simultaneous study of the superparamagnetic and optical properties of these magnetic photocatalytic nanocomplexes and the determination of the influence of oxygen vacancies on these properties is also a contribution. It should be noted that if we compare the existing literature data, the influence of oxygen vacancies was specifically studied, but for another photocatalyst, ZnO, and only partially, since the optical absorption spectra were not studied [11].

II. EXPERIMENTAL PROCEDURE

TiO_2 nanopowders coated by Ni clusters were obtained by a novel technology of metallic cluster deposition on a fine TiO_2 nanopowder with a mean grain size of 25 nm (Degussa AG) developed at the Andronikashvili Institute of Physics of Ivane Javakhishvili Tbilisi State University. The technology is electroless and inexpensive. It proceeds at low temperatures (50-60^{o}C) and hence does not lead to changes of the physical properties of the material to be coated nor of the material of clusters [12-14].

The composition of the chemical solution for obtaining of TiO_2/Ni nanopowder is: $NiSO_4 \cdot 6H_2O$ 30 g/l that provides the Ni ions, $KNaC_4H_4O_6$ $4H_2O$ - 40 g/l is a complexing agent preventing the excess of free metal ions concentration, ethylenediamine-15 g/l is a cross-linker, and NaOH - 40 g/l, regenerative borohydride $NaBH_4$-6 g/l. The excess amount of borohydride causes the solution to decay and the precipitation of metallic Ni in the solution. At the end of the process, the solution is transparent, which confirms the precipitation of the bulk of the nickel from the solution. The same method was applied for the preparation of TiO_2/Co powders: an aqueous cobalt solution containing: $CoSO_4 \cdot 7H_2O$ – 5 g/L, $C_{10}H_{16}N_2O_8$ (ethylenediaminetetraacetic acid, EDTA, Trilon B) – 35 g/L, NaOH – 40 g/L (giving a pH of 13 after TiO_2 addition), $NaBH_4$ was added (in aqueous solution to give a concentration of 0.5–5 g/L) after suspending the TiO_2 (0.5 g per 100 mL solution) in the solution. Thereafter the suspension was treated by ultrasound for 20 min and then stirred by a magnetic bar during heating (75–80°C). The amount of borohydride and the duration of the reaction determine the quantity of the deposited cobalt. The decorated particles were separated from the solution by centrifuging and were dried in the air. The characteristics of the chemicals used are given in Table I.

TABLE I. PURITY OF THE CHEMICALS USED FROM MANUFACTURER WITHOUT ADDITIONAL PURIFICATION

Name	Purity	Manufacturer
TiO_2 anataze, 44 μm	99%	Sigma-Aldrich
TiO_2 anatase, 30nm	99.98%	Us-nano
TiO_2 anatase, 5-10 nm	99%	Sun-nano
P 25, 30-35 nm	99%	Degussa
$NiSO_4 \times 6H_2O$	98.5%	Sigma-Aldrich
$NaBH_4$	99%	Sigma-Aldrich
NaOH	99%	Sigma-Aldrich
$KNaC_4H_4O_6 \bullet 4H_2O$	99.18%	JSC Base No. 1 of Chemical Reactives
$CoSO_4 \cdot 7H_2O$	99%	Sigma-Aldrich
Ethylenediamine EDTA	99%	Sigma-Aldrich

The concentration of the suspensions used in the optical studies was 5 mg of powder per 600 ml of distillate. It was observed in the experiments that the ratio of light absorption by suspensions to scattering depends on the concentration of the suspension, and it is maximal for suspensions with a concentration of about 5/600 mg/ml. That is why suspensions of the mentioned concentration were used in the experiments in order to make the absorption peaks shown on the absorption curves sharper.

Magnetization measurements were carried out using a Vibrating Sample Magnetometer - VSM (Cryogenic Limited, UK) allowing one to do magnetization measurements in a wide range of temperature 1.7 ÷ 293 K and in Zero-magnetic Field Cooling (ZFC) and magnetic Field Cooling (FC) modes. At ZFC mode, a sample is first cooled down to 1.7 K in a zero magnetic field and then the sample is heated in a small magnetic field up to room temperature. Measurements are

taken to obtain the sample-blocking temperature T_B related to the magnetic anisotropy of the nanoparticles. The application of an external field introduces the competition between the spin orientation along the magnetic anisotropy axis and the direction of the magnetic field under the action of thermal fluctuations. Small applied fields (≤500 Oe) are generally insufficient to induce spin reorientation away from the anisotropy axis at low temperature, with increasing temperature, however, thermal activation assists in the orientation of the magnetic moments into the direction of the magnetic field magnetizing a sample. The recorded magnetization passes through a maximum before it is reduced again at higher temperatures due to thermally induced reversals of the particle magnetization vectors according to the Curie law in the superparamagnetic magnetic state above the blocking temperature T_B. Due to the laboriousness of VSM measurements, the homemade Radio-Frequency (RF) resonant magnetometer (RF RM) was also used to characterize the magnetic properties of the received samples, allowing one to carry out more easily and quickly assess of the magnetic state (ferromagnetic, superparamagnetic) of the tested sample compared to the comparatively long-term measurements by the VSM magnetometry [15]. The circuit based on the LC resonance generator (Figures 2-3) is used for the measurements of the transverse susceptibility of magnetic samples.

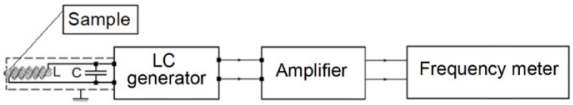

Fig. 2. Circuit based on the LC resonance generator.

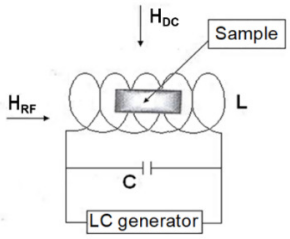

Fig. 3. LC generator circuit scheme.

The sample was placed into the induction coil of the LC generator. The variations of its resonance frequency were measured at the variations in the external magnetic field H_{DC}, which was perpendicular to the coil field H_{RF}. The standard representation of the frequency of the LC generator oscillations is:

$$f = \frac{1}{2\pi\sqrt{LC}} \quad (1)$$

where L is the coil inductance and C is its capacity.

The introduction of the sample into the induction coil changed the inductance value by ΔL. If $\Delta L/L << 1$, by differentiating this equation, we get:

$$\frac{\Delta f}{f} = -\frac{\Delta L}{2L} \quad (2)$$

The inductance variations are connected with the changes in the magnetic susceptibility of the studied magnetic nanopowders. The semiconductor powder coated with metallic clusters obtained by the electroless method is placed in the capsule and the magnetic characteristics are measured using the above methods. Then optical and EPR measurements are performed.

The optical absorption spectra of the distillate suspensions of the photocatalyst powders were measured. First, the light absorption of the distilled water over the entire working spectral range was studied and appeared to be rather low. However, in order to exclude the distortion of the absorption spectra of the powders under study as a result of the distillate effect, we recorded the absorption spectra of the powders dissolved in the distillate in reference to the pure distillate. For this aim, a cell with a suspension of the powder under study was placed in one compartment of the spectrophotometer F-46 and an identical cell with pure distillate in another compartment. To check the validity of the procedure, we prepared several similar reference aqueous suspensions of the same powder. Then their absorption curves were taken. The obtained spectra coincided very closely with a maximum difference of ± 5 %. EPR spectra were recorded by spectrometer EPR-V (Russia), with 9.1 GHz microwave frequency and 100 KHz magnetic field modulation frequency. Experiments were carried out with microwave power of 15 mW. As an EPR standard, MgO doped with Mn^{2+} ions was used. The values of hyperfine splitting and g-factor were measured by means of EPR standard.

III. RESULTS AND DISCUSSION

A. *Magnetic and Photocatalytic Properties of the Ni-coated TiO_2 Nanopowders*

The results of VSM magnetization measurements for two types of TiO_2/Ni nanopowders obtained as a result of TiO_2 nanopowder coating for 10 and 1 min are presented in Figures 4-8.

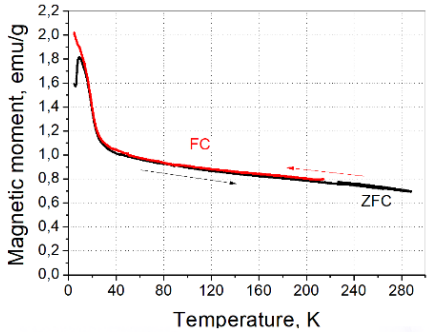

Fig. 4. Temperature dependence of the zero-field-cooled (ZFC) and field-cooled (FC) magnetic moments of the anatase TiO_2 nanopowder coated by Ni clusters. Deposition time: 10 min. Applied magnetic field: 1000 Oe.

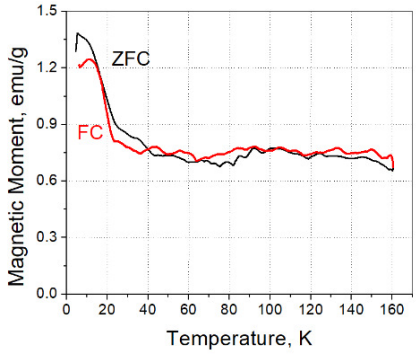

Fig. 5. Temperature dependence of the ZFC magnetic moment of the anatase TiO_2 nanopowder coated by Ni clusters with deposition time of 1 min in applied magnetic field of 1000 Oe.

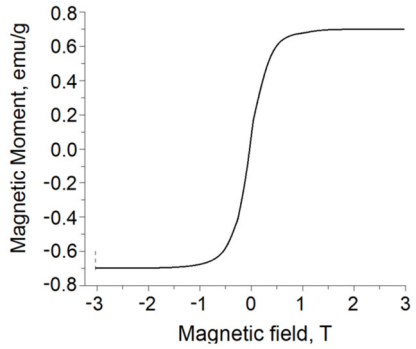

Fig. 6. Hysteresis loop for the anatase TiO_2 nanopowder coated by Ni nanoclusters for 10 min at T=260 K.

The results of the VSM measurements are confirmed by the RF RM measurements (Figure 7). Absence of hysteresis at up-and-down scanning of the magnetic field is observed, indicating that deposited nickel clusters are superparamagnetic. By making appropriate measurements at nitrogen temperature, it is easy to establish whether below T=77 K or above this temperature the blocking temperature T_B of the superparamagnetic coating is located. Figures 7 and 8 show the possibility of controlling the magnetization of nanoclusters by the RF RM method depending on the duration of the reduction reaction and the concentration of the reducing agent.

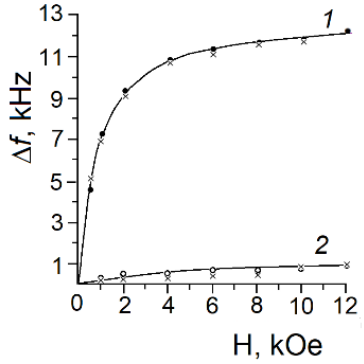

Fig. 7. RF resonant magnetometer frequency f change Δf dependence (f =7 MHz at H=0) at room temperature on the magnetic field strength ((•) and (×) mark up and down magnetic field sweeps) for: *1* – Ni coated anatase TiO_2, reaction duration 10 min and *2* – Ni coated anatase TiO_2, reaction duration 30 s.

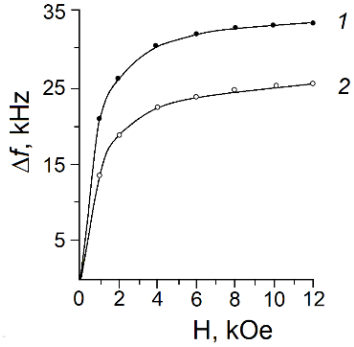

Fig. 8. Dependence of the frequency deviation Δf of the RF resonant magnetometer on the magnitude of the external magnetic field depending on the concentration of the reducing agent: *1* – TiO_2/Ni, reducing agent concentration 3 g/l and *2* – TiO_2/Ni, reducing agent concentration 1 g/l.

The characteristic features of the magnetization data in Figures 4 and 5 are the peaks on the ZFC magnetic moment temperature dependences. Such peaks are known to be characteristic for the superparamagnetic particles and were observed in order to obtain the blocking temperatures of the samples to characterize the magnetic anisotropy of the particles [16]. Therefore, we conclude that the obtained nanopowders become superparamagnetic due to the presence of Ni clusters on the surface of TiO_2/Ni nanopowders. From the position of the ZFC peaks at 1000 G the blocking temperatures T_B are about 9 and 6 K, respectively. The superparamagnetic behavior of samples can also be seen from the curves in Figure 7 due to the absence of hysteresis. In the case of low signal intensity when measuring with the RF RM method, the more sensitive EPR method [9] can be used.

For testing the efficiency of the developed nanotechnology of deposition of Ni clusters on photocatalytic TiO_2 nanopowders, we took two modifications of the TiO_2 powder, anatase and rutile, with grains of ~ 30 nm in size. We prepared their identical suspensions in distillate and recorded their absorption spectra over the wavelength range from 300 to 800 nm. Then we deposited Ni clusters on the powders under study and recorded again their absorption spectra over the same wavelength range by the same technique. Figure 9 shows the results of these experiments: curve *1* corresponds to the absorption spectrum of rutile modification of the TiO_2 powder before deposition of clusters, after deposition of clusters the spectrum hardly changed and it is omitted. Curve *2* corresponds to the absorption spectrum of the anatase modification of the TiO_2 powder before the deposition of clusters, and curve *3* to that after the deposition of the clusters. Curves *1* and *2* showed that the absorption spectra of the rutile and anatase modifications before the deposition of Ni clusters were very much alike, without any particular absorption at any wavelength. After the deposition of the clusters, the absorption spectrum of the rutile modification did not change, as was mentioned above, but the spectrum of the anatase modification changed dramatically, as curve *3* showed. The observed phenomenon is apparently caused by the fact that, before the deposition of clusters, the electron-hole pairs recombine fast on the nanoparticle surfaces, but, after the deposition of clusters, they capture the electrons and hinder the recombination. As a result, in the process of photocatalysis the number of split

water molecules increases, improving the efficiency of the photocatalytic reaction. The results on the dependence of the TiO_2/Ni nanopowder absorption spectra on the Ni deposition time are presented in Figure 10.

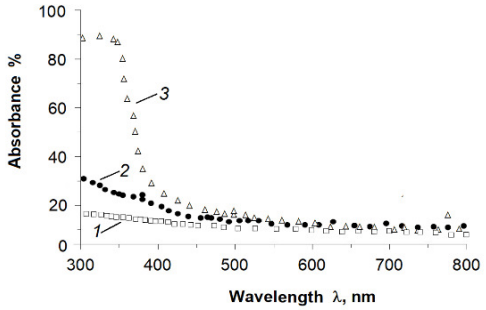

Fig. 9. Absorption spectra of TiO_2 nanopowders before and after coating with Ni clusters: *1*- absorption spectra of nanopowders TiO_2 (rutile) before coating with Ni clusters, *2*- absorption spectra of nanopowders TiO_2 (anatase) before coating with Ni clusters, *3*- absorption spectra of nanopowders TiO_2 (anatase) after coating with Ni clusters.

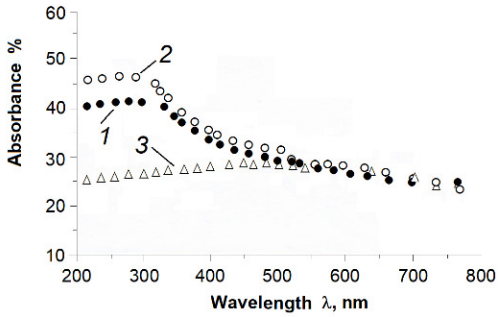

Fig. 10. TiO_2 (Anatase) nanopowder absorption spectra dependence on deposition time: *1* – pure TiO_2, *2* – TiO_2 coated with Ni for 1 min, *3* – TiO_2 coated with Ni for 10 min.

As seen from Figure 10, after some increase in absorption with deposition time, the decrease observed in the 200-500 nm wavelength range is apparently due to the increased coverage of TiO_2 nanoparticle surfaces by Ni nanoclusters. Figure 11 shows the optical absorption spectra of TiO_2 (P25) nanopowders (TiO_2 (Degussa P25)), anatase – 86%/rutile - 14%)) with mean grain size of 25 nm before and after the coating by Ni nanoclusters. As can be seen from Figure 11, the optical absorption increases as a result of cluster deposition on TiO_2 (P25) nanopowder only in the short length wave interval of 200-400 nm. So, TiO_2 (P25) nanopowders with Ni nanocluster coatings should be more suitable for photocatalysis, not only because of the larger specific surface area, but also due to the higher specific efficiency of the surface. EPR study of the photocatalytic activity of TiO_2/Ni nanopowders was also carried out [8].

B. Magnetic and PhotocatalyticPproperties of the Co-coated TiO_2 Nanopowders

In Figure 12, the results of the VSM magnetization measurements are presented for two types of TiO_2/Co nanopowders obtained as a result of TiO_2 nanopowder coating reaction for 1 min and full reaction, respectively.

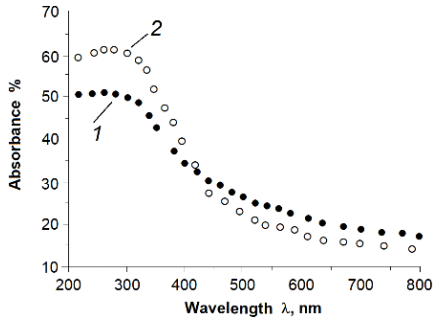

Fig. 11. The absorption spectrum changes of TiO_2 (P25) nanopowders with 25 nm particle size as a result of Ni cluster coating: *1* - TiO_2 (P25) absorption spectrum before Ni cluster coating and *2* - TiO_2 (P25) absorption spectrum after Ni cluster coating.

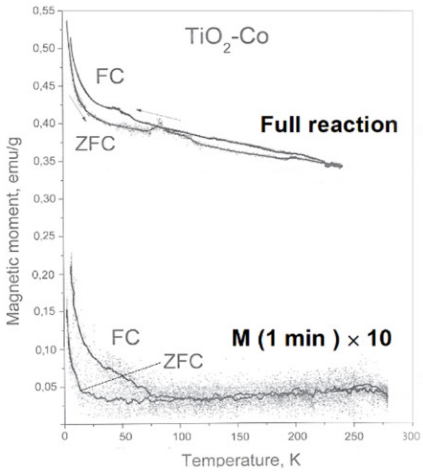

Fig. 12. ZFC and FC magnetization dependence on reaction duration (reducer concentration 5g/l). The applied magnetic field is 1000 Oe.

One can see an increase in the magnetization by almost 50 times and the dependence of the magnetization of the Curie law type with a small hysteresis in the temperature dependence. The annealing of a full reaction sample at 600°C completely transforms this dependence as shown in Figures 13-16.

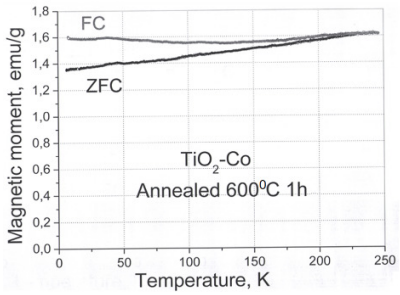

Fig. 13. Temperature dependence of the ZFC and FC magnetic moments of the TiO_2 nanopowder coated by Co clusters after annealing at 600°C for 1 hr. The applied magnetic field is 1000 Oe.

The analysis of the obtained results and the literature shows that Curie law type magnetization dependence of samples in Figure 12, characteristic for CoO, after annealing transforms in a magnetization dependence characteristic for nanocrystalline

superparamagnetic cobalt Co with comparatively high blocking temperatures as compared with the nickel coated samples of Figures 4-5. RF RM measurements at up and down magnetic field sweeps (Figure 16) show the superparamagnetic behavior at T=300 K and ferromagnetic one at T=77 K.

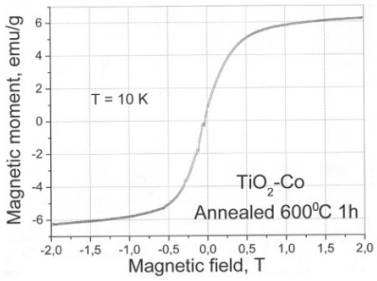

Fig. 14. Hysteresis loop for the TiO_2 nanopowder coated by Co nanoclusters after the annealing at 600°C for 1 hr at T=10 K.

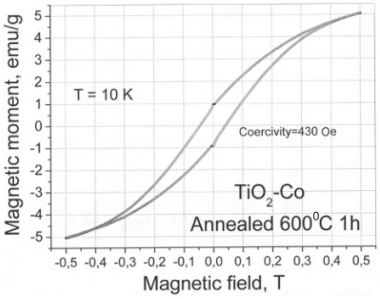

Fig. 15. Hysteresis loop for TiO_2 nanopowder coated by Co nanoclusters after the annealing for 1 hr at T=10 K. Coercivity is 430 Oe.

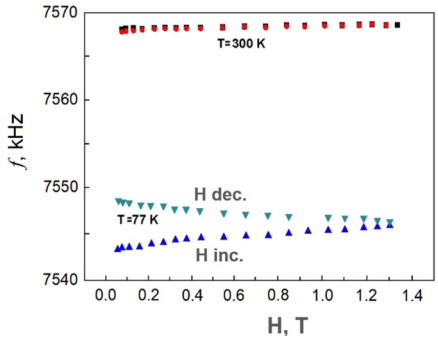

Fig. 16. RF RM measurements at up and down magnetic field sweeps at T=300 K and at T=77 K.

Cluster concentration by changing the reaction duration was controlled by the resonant sizes coated on the TiO_2 surface. It could be regulated by choosing the restoration agent magnetometer measurements. For example, Figure 17 shows a series of resonant magnetometer curves at different reaction durations, while the reducer concentration was 5 g/l. The changes in the magnetic characteristics by selecting the reducer concentration in the aqueous solution of cobalt nanoparticles were studied also, the result can be seen in Figure 18. The result was expected. As the reducer concentration increases, the thickness of the coated cluster increases and enhances their magnetization.

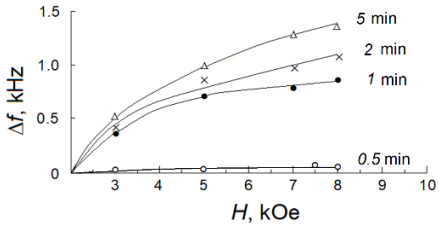

Fig. 17. Frequency deviation $\Delta f(H)$ for different durations of Co cluster coating (captions on curves), at reducer concentration of 5 g/l.

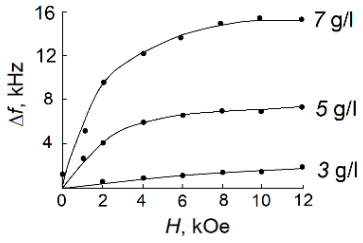

Fig. 18. Frequency deviation $\Delta f(H)$ (f =8.5 MHz when H = 0) at room temperature. (•) at sweeping of the magnetic field for the three different concentrations of the reducer (3 g/l, 5 g/l, and 7 g/l) at full reaction time.

Figure 19 shows the results of EPR measurements of Co deposited TiO_2. Nanopowders are presented depending on the Co deposition time in the solution.

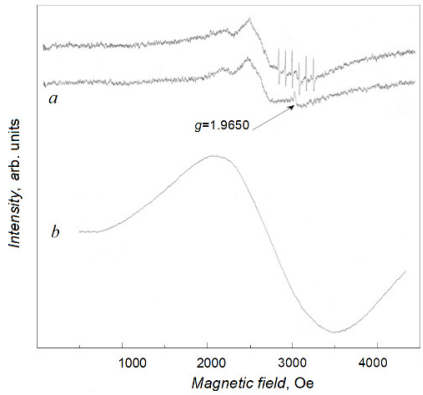

Fig. 19. EPR measurements of Co deposited TiO_2: (a) Co cluster, deposition time 30 s and (*b*) Co cluster deposition time 5 min.

At short deposition time (Figure 19) two resonances can be seen: one corresponding to oxygen vacancies (g = 1.9650) and one to Co nanoclusters. At long deposition time, one could see apparently a strong resonance line corresponding to the room temperature superparamagnetic state formed by Co clusters and oxygen vacancies [9]. It was found that the optimal time for Co-deposition is 20 s. It is also confirmed by the analysis of the optical absorption spectra and EPR spectra [8].

In the conducted experiments, changing the coating duration we can regulate the nanoclusters size, and consequently, the magnetic properties of the nanoparticles powders coated with clusters.

Figure 20(a) shows the optical absorption spectra of TiO_2 powder with grain size of 44 μm where curve 1 corresponds to the absorption spectrum of the TiO_2 powder without Co clusters, and curve 2 to the absorption spectrum with deposited Co clusters. As can be seen from Figure 20(a), the optical absorption only slightly increases as a result of cluster deposition. This indicates that the majority of the created electrons and holes annihilate before they reach the TiO_2 grain surface, i.e. the annihilation occurs in the powder particle volume, and hence the deposition of clusters on the surface has no significant effect. Thus, we can conclude that micron-sized powders not only have a small specific area, but also the specific efficiency (efficiency per area unit) of the surface itself is low. Therefore, the micron-sized TiO_2 powder is not an efficient photocatalyst. The nanosize Co coated TiO_2 powders can be more effective for photocatalytic applications. To check this possibility, we deposited Co clusters on nanosize (5-10 nm) TiO_2 powders.

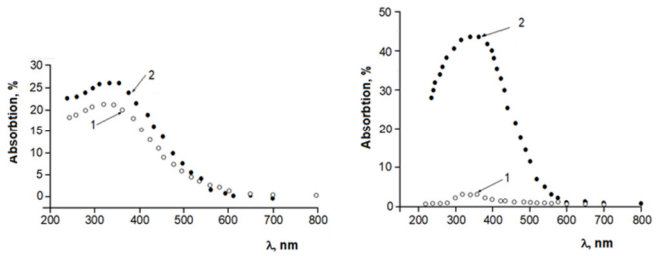

Fig. 20. The effect of Co nanoclusters on the optical absorption spectra of TiO_2 powders with different grain sizes: (a) 44 μm and (b) 5-10 nm. Curves 1 and 2 correspond to the absorption spectrum of the TiO_2 powder without and with Co clusters, respectively.

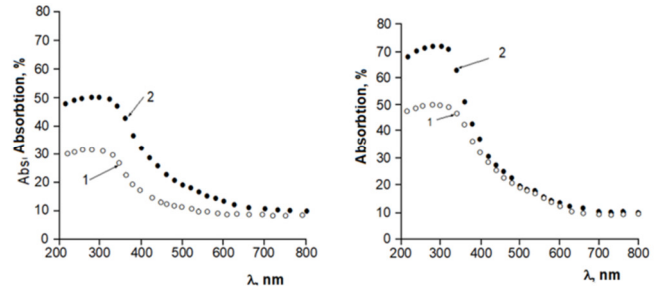

Fig. 21. Optical spectra of commercial TiO_2 powders and the effect of nanocluster deposition. (a) 30-35 nm size commercial TiO_2 nanopowders optical spectra: 1 - anatase, 2 - P25 (86 % anatase, 16% rutile), (b) change of the optical spectrum of P25 in the result of Co cluster coating: 1 – Optical spectrum before deposition of clusters, 2 – Optical spectrum after deposition of Co clusters.

Figure 20(b) shows the optical absorption spectra of TiO_2 nanopowder with and without Co cluster coating. As can be seen by the comparison of Figures 20(a) and (b), the light absorption of TiO_2 without Co deposition in nanopowder is much smaller than in micropowder. However, the deposition of Co clusters leads to a huge increase of the light absorption in the nanopowder sample, while the effect as we have seen was small in micropowder. The obtained results show that TiO_2 nanopowder with Co cluster coating is more suitable for photocatalysis, not only because of the larger specific surface area, but also due to the higher specific efficiency of surface compared to the micropowder.

The maximal effect of Co cluster deposition on TiO_2 nanopowders was obtained in the case of 30-35 nm size nanopowders, when the clusters were deposited not on the pure anatase modification of TiO_2, but on the anatase and rutile mixture (86% anatase, 14% rutile), called P25. Figure 21 shows the absorption spectra of anatase with 30-35 nm nanoparticles and P25 before and after the deposition of Co clusters. As a result of the deposition, curve 1 corresponds to the absorption spectrum before the Co-cluster deposition, and curve 2 - after the Co-cluster deposition. As can be clearly seen, the increase of light absorption is significant in the ultraviolet area. Thus, using a mixture of modified anatase and rutile as a starting material instead of pure anatase and depositing the powder grain surfaces by cobalt nanoclusters, it is possible to significantly increase the TiO_2 efficiency in the ultraviolet field in view of the separation of the photo-induced charges, that is the starting stage for the entire photocatalysis process.

The next step in the photocatalyst process, which requires an increase in the efficiency of oxide photocatalysts, among them TiO_2, is the use of visible light for photocatalysis. Figure 22 shows the change of optical spectrum of P25 after the deposition of Co clusters and thermal treatment in a vacuum furnace.

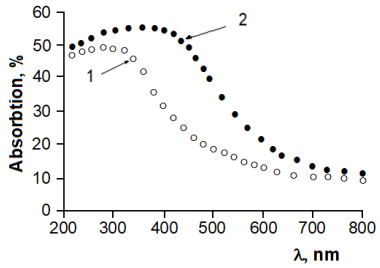

Fig. 22. Change of the optical spectrum of TiO_2(P25) after complex treatment. 1 – optical spectrum of the commercial P25, 2 - optical spectrum of the commercial P25 after Co-cluster deposition and vacuum thermal treatment.

Curve 1 corresponds to the optical spectrum of commercial P25 and curve 2 corresponds to the optical spectrum of P25 after the cobalt cluster deposition and vacuum thermal treatment. Thermal treatment was carried out in a vacuum furnace at 600 ^{0}C for 7 hr. As can be seen from the Figure, the absorption spectrum shifts in the visible light area, causing the improvement of using visible light during the photocatalysis process and thus increasing this efficiency. It is clear that the reason for this is the modification of the energy gap, possibly caused by the diffusion of cobalt atoms in TiO_2 nanoparticle volume and the creation of impurity levels. As recent studies indicate, the observed effect is also associated with an increase in the number of oxygen vacancies that are formed in the samples during vacuum annealing at high temperatures [17].

Thus, the complex processing of titanium dioxide nanopowders by cobalt cluster deposition and then vacuum thermal treatment can improve its photocatalytic properties.

IV. CONCLUSIONS

TiO_2 nanopowders coated with Ni and Co nanoclusters with higher light absorption and enhanced photocatalytic activity were synthesized for the first time via an original facile electroless method. Magnetization measurements demonstrated the superparamagnetic behavior of the obtained TiO_2/Ni nanopowders and TiO_2/Co nanopowders after annealing. They confirm that nanosized Ni and Co nanoclusters are deposited on the surface of TiO_2 grains. The reasons for different changes in properties of TiO_2/Ni and TiO_2/Co magnetic nanocomplexes after annealing were explained. The photocatalytic properties of TiO_2 powder were also studied with EPR spectroscopy. The nature of the dependence of the EPR spectra on the size of magnetic clusters is established. Optical spectroscopy measurements showed a significant increase of light absorption in Ni- and Co-coated TiO_2 nanopowders, mainly in the ultraviolet region. It was found that the deposition of Ni, Co nanoclusters on the TiO_2-P25 nanopowder provides the best results and the optimal deposition time was determined to be 20 s. As a result of the vacuum heat treatment, a significant increase in absorption was observed in the visible region as well. This increase should be attributed to the appearance of impurity levels in the energy spectrum of titanium oxide, which occurs as a result of the diffusion of impurity atoms from clusters in the volume of this oxide at high temperatures. It is discussed that, in accordance with our recent results, oxygen vacancies, which arise as a result of the vacuum heat treatment at high temperatures, play an important role in the observed increase in light absorption. The facile and fast method presented in the present study can be generally applied to coat different materials with transition metal nanoclusters to develop efficient sun light-driven photocatalysts.

ACKNOWLEDGMENT

This work was supported by Shota Rustaveli National Science Foundation of Georgia (SRNSFG) [FR-21-9263].

REFERENCES

[1] M. Audin and M. Kaneko, *Photocatalysis*. Tokyo, Japan: Springer, 2002.

[2] S. Peiris, H. B. de Silva, K. N. Ranasinghe, S. V. Bandara, and I. R. Perera, "Recent development and future prospects of TiO2 photocatalysis," *Journal of the Chinese Chemical Society*, vol. 68, no. 5, pp. 738–769, 2021, https://doi.org/10.1002/jccs.202000465.

[3] R. M. Navarro, F. del Valle, J. A. Villoria de la Mano, M. C. Álvarez-Galván, and J. L. G. Fierro, "Photocatalytic Water Splitting Under Visible Light: Concept and Catalysts Development," in *Advances in Chemical Engineering*, vol. 36, H. I. de Lasa and B. Serrano Rosales, Eds. Academic Press, 2009, pp. 111–143.

[4] L. Lin, T. Hisatomi, S. Chen, T. Takata, and K. Domen, "Visible-Light-Driven Photocatalytic Water Splitting: Recent Progress and Challenges," *Trends in Chemistry*, vol. 2, no. 9, pp. 813–824, Sep. 2020, https://doi.org/10.1016/j.trechm.2020.06.006.

[5] H. A. Maddah, "Numerical analysis for the oxidation of phenol with TiO_2 in wastewater photocatalytic reactors," *Engineering, Technology & Applied Science Research*, vol. 8, no. 5, pp. 3463-3469, Oct. 2018, https://doi.org/10.48084/etasr.2304

[6] M. Mahshidnia and A. Jafarian, "Forecasting wastewater treatment results with an ANFIS intelligent system", *Engineering, Technology & Applied Science Research*, vol. 6, no. 5, pp. 1175-1181, Oct. 2016, https://doi.org/10.48084/etasr.745

[7] M. Nadareishvili, G. Mamniashvili, D. Jishiashvili, G. Abramishvili, C. Ramana, and J. Ramsden, "Investigation of the visible light sensitive ZnO photocatalytic thin films," *Engineering, Technology & Applied Science Research*, vol. 10, no. 2, pp. 5524-5527, Apr. 2020, https://doi.org/10.48084/etasr.3392

[8] D. Japaridze *et al.*, "Magnetic Properties and Photocatalytic Activity of the TiO2 Micropowders and Nanopowders Coated by Ni Nanoclusters," *Journal of Superconductivity and Novel Magnetism*, vol. 32, no. 10, pp. 3211–3216, Oct. 2019, https://doi.org/10.1007/s10948-019-5088-2.

[9] M. Nadareishvili *et al.*, "Decoration of photocatalytic TiO2 particles by cobalt clusters," *Nanotechnology Perceptions*, vol. 16, no. 3, pp. 336–347, Nov. 2020.

[10] T. Gavasheli, G. Mamniashvili, M. Nadareishvili, and T. Zedginidze, "Electroless Technology for Production of Cobalt Magnetic and Photocatalytic Nanopowders and Nanowires," *TechConnect Briefs*, vol. 2019, pp. 42–45, Jun. 2019.

[11] Q. Zhang, M. Xu, B. You, Q. Zhang, H. Yuan, and K.Ostrikov, "Oxygen Vacancy-Mediated ZnO Nanoparticle Photocatalyst for Degradation of Methylene Blue," *Applied Sciences*, vol. 8, no. 3, Mar. 2018, Art. no. 353, https://doi.org/10.3390/app8030353.

[12] T. N. Khoperia, T. Zedginidze, K. Kvavadze, and M. Nadareishvili, "Development of competitive nanotechnologies for solution of challenges in photocatalysis, electronics and composites fabrication," *ECS Meeting Abstracts*, no. 2, 2007, Art. no. 107.

[13] T. N. Khoperia, T. I. Zedginidze, and T. Gegechkori, "Magnetic and Catalytic Properties of Electroless Nickel, Ni-P and Ni-P-Re Thin Films," *ECS Transactions*, vol. 25, no. 24, Feb. 2010, Art. no. 97, https://doi.org/10.1149/1.3316118.

[14] T. Khoperia, G. Mamniashvili, M. Nadareishvili, and T. Zedginidze, "Competitive Nanotechnology for Deposition of Films and Fabrication of Powder-Like Particles," *ECS Transactions*, vol. 35, no. 10, Oct. 2011, Art. no. 17, https://doi.org/10.1149/1.3640401.

[15] G. I. Mamniashvili *et al.*, "Magnetometry and Hyperthermia Study of Magnetic Fluid Preparation UNIMAG," *World Journal of Condensed Matter Physics*, vol. 4, no. 1, pp. 6–12, Feb. 2014, https://doi.org/10.4236/wjcmp.2014.41002.

[16] G. C. Papaefthymiou, "Nanoparticle magnetism," *Nano Today*, vol. 4, no. 5, pp. 438–447, Oct. 2009, https://doi.org/10.1016/j.nantod.2009.08.006.

[17] M. Nadareishvili, T. Zedginidze, and E. Chikvaidze, "On the Possibility of Improving the Efficiency of Oxide Photocatalysts," in *IV International scientific and practical conference "Scientific progress: innovations, achievements and prospects*, Munich, Germany, 2023, pp. 138–141.